Journal of Chemical Technology and Biotechnology 93 (2018): 2262-2270

DOI: http://doi.org/10.1002/jctb.5569

Two-step persulfate and Fenton oxidation of naphthenic acids in water

Xiyan Xu[a,b]*; Gema Pliego[a]; Juan A. Zazo[a]; Shuming Liu[b]; Jose A. Casas[a]; Juan J. Rodriguez[a]

[a] *Chemical Engineering Section, University Autonoma of Madrid, Crta. Colmenar km 15, 28049 Madrid, Spain*

[b] *School of Environment, Tsinghua University, 100084, Beijing, China*

**Corresponding author:*

E-mail address: yorkxxu@gmail.com

ABSTRACT

BACKGROUD: In the current study, two-step persulfate and Fenton oxidation has been investigated for the mineralization of naphthenic acids at 80 ^{o}C and initial pH ≈ 8. This pH evolves during the persulfate oxidation step towards the optimum for Fenton oxidation (≈ 3). The effects of persulfate and H_2O_2 doses, iron concentration, duration of the persulfate oxidation step and operating temperature have been assessed.

RESULTS: The combined treatment allowed up to ≈ 80% mineralization of cyclohexanoic acid using fairly low relative amounts of reagents (20 and 30% of the stoichiometric for persulfate and H_2O_2, respectively). For mineralization of cyclohexanoic acid, 115 and 87 kJ mol^{-1} were obtained as representative values of the apparent activation energy for the persulfate and Fenton oxidation steps, respectively. The system was also successfully tested with other naphthenic acids, including cyclohexanebutyric acid, 2-naphthoic acid and 1,2,3,4-tetrahydro-2-naphthoic acid. Treatment of the naphthenic acids tested by this system gave rise to easily biodegradable

This article has been accepted for publication and undergone full peer review but has not been through the copyediting, typesetting, pagination and proofreading process, which may lead to differences between this version and the Version of Record. Please cite this article as doi: 10.1002/jctb.5569

effluents consisting mainly of short-chain organic acids. The biodegradability was confirmed by the BOD_5/COD ratio and respirometric tests.

CONCLUSION: The results show the potential application of this approach as a promising cost-effective solution for the treatment of naphthenic acids-bearing aqueous wastes. This approach has significant advantage compared to the single thermally-activated persulfate or Fenton oxidation, since it allows a high mineralization at reduced reagent cost upon replacing part of the persulfate by less expensive H_2O_2.

Key words: Naphthenic acids; Persulfate; Fenton; Oxidation; Mineralization; Biodegradability.

INTRODUCTION

The negative environmental impacts of naphthenic acids (NAs) raise increasing attention[1-4]. NAs have been reported as persistent pollutants present in marine oil spills[5] and oil sands processes-affected wastewaters (OSPWs) with high toxicity toward a wide variety of organisms, including microorganisms, plants and animals[6-8]. NAs are carboxylic acids including in their structure aromatic and naphthenic rings together with aliphatic chains in lower proportion. They can be represented by a common chemical formula of $C_nH_{2n+Z}O_2$[9], but also include some diacids, keto- and heteroatomic groups[10]. In addition, positional and stereo isomerism of alicyclic NAs result in numerous cis-/trans isomers, and the branching of acyclic NAs can even further increase their complexity[11]. Surrogate model NAs, such as cyclohexanoic acid (CHA), are used to investigate their environmental-related features[12, 13].

Different techniques addressed to the removal of NAs from aqueous wastes have been investigated[14]. Those include adsorption[15], biodegradation[16] and advanced oxidation processes (AOPs)[9, 17, 18]. Adsorption, being a non-destructive operation, gives rise to secondary wastes while conventional biological treatments are limited by the toxicity and recalcitrant character of NAs[2]. AOPs have proved their ability for the mineralization of a wide diversity of target organics. H_2O_2 and persulfate (PS) are known precursors of hydroxyl ($HO^{\bullet}$) and sulfate ($SO_4^{\bullet-}$) radicals, under the action of different catalytic agents, like activated carbon[19], metals[20, 21] and their oxides[22], or by some energy source, including thermal[23], light (UV[24, 25]/solar[26]/LED[27]) and electricity[28]. NAs have been degraded by ozonation[29], thermally-activated PS[12], zero valent iron (ZVI)-activated PS[9], UV/PS, UV/H_2O_2, chelate-Fenton[30], UV(solar)/TiO_2[18, 31] and UV/Chlorine[32]. $HO^{\bullet}$ radicals preferentially attack the α position of the aliphatic chains and the para-position of the naphthenic ring of CHA[17], while $SO_4^{\bullet-}$ radicals are believed to firstly cause the decarboxylation of CHA[9, 33].

Our previous work demonstrated that thermally-activated PS oxidation can efficiently cause the mineralization of NAs with dissolved oxygen participating as oxidizing species[12]. The reaction between NAs and sulfate radicals generated from thermal activation of PS give rise to the corresponding organic radicals which can react with oxygen yielding reactive $O_2^{\bullet-}$/$HO_2^{\bullet}$[12, 34-36]. However, the drawbacks of PS-based approach, including the introduction of sulfur species and most particularly the high reagent cost, hinders its potential application.

Fenton oxidation is one of the main AOP systems and has been recognized as a cost-effective solution for a number of industrial wastewaters compared to the PS-based ones[37, 38]. It uses H_2O_2 as starting reagent and Fe^{2+} as catalyst, which promotes the generation of strongly oxidizing hydroxyl radicals. The Fenton process can also be

intensified by increasing the temperature (i.e. high temperature Fenton, HTF)[39, 40]. However, Fenton oxidation has been rarely attempted for NAs breakdown, due partially to the basic pH of the OSPWs containing NAs[9, 18] and also to the complexation of Fe ions by NAs which hinders their activity[41]. In fact, several efforts have been made to adapt the Fenton-based technology to a wider range of pH[42]. Recently, Zhang et al.[13, 30, 43] used chelate-Fenton systems to treat CHA at basic pH. However, the scavenging effect of the chelate agents toward $HO^{\bullet}$ radicals represents a main drawback regarding H_2O_2 consumption and on the other hand it has to be considered the possible increase of toxicity derived from them and/or their degradation byproducts.

The as-generated OSPWs containing NAs are commonly characterized by a moderately basic pH (≈ 8) and a temperature well above the ambient (≈ 80 ^{o}C), as used in the oil sand extraction process[2, 44]. The reactions involved in PS oxidation yield important amounts of protons[9, 19], thus giving rise to strong decrease of pH. Therefore, a treatment based on thermally-activated PS oxidation followed by Fenton to deal with NAs from OSPWs could achieve several objectives. The first step allows NAs breakdown with significant mineralization[12], thus avoiding Fe-NA complexation. The effluent from this step would also reduce the Fe-NA complexation in the following Fenton step. On the other hand, during PS oxidation, the pH decreases down to the optimum range for the Fenton process. A convenient combination of those two AOPs could provide a high mineralization of NAs giving rise to a final effluent of low toxicity and easily biodegradable at much lower cost by replacing part of the PS by cheaper H_2O_2. Moreover, the need of acidifying agents for the Fenton process is avoided.

The aim of this study is to assess the efficiency of this approach for the abatement of model NAs, namely cyclohexanoic acid (CHA), cyclohexanebutyric acid (CHBA), 2-naphthoic acid (2-NA) and 1,2,3,4-tetrahydro-2-naphthoic acid (1234-T-2-NA), which

include naphthenic ring and aromatic structures[12]. CHA was used as model compound to study the effect of the operating variables as well as the kinetics of mineralization. The biodegradation of the effluents from the treatment of the NAs tested was also studied.

MATERIALS AND METHODS

Experimental procedures

The two-step PS and Fenton oxidation experiments were carried out in batch, in 100 mL stoppered glass flasks placed in a constant-temperature water bath with a shacking frequency equivalent to 200 rpm. In each run, 50 mL of aqueous solution of the NAs tested (CHA, CHBA, 2-NA and 1234-T-2-NA, purity over 98%, purchased from Sigma-Aldrich) were preheated for over 15 min at different temperatures (60−97 ^{o}C ± 1) after adjusting the pH to 8 by adding proper amount of NaOH solution (in distilled water) with concentration of 1 M. The pH value of the solution was not artificially controlled upon the reactions. Then, sodium persulfate (1−20% of the stoichiometric amount) was added to start the PS oxidation stage. After a given reaction time (0.5−2 h), H_2O_2 (10−80% of the stoichiometric) and Fe^{2+} (0.5−20 mg L^{-1}, using $FeSO_4$•$7H_2O$) were added simultaneously for reaction during another 4 h. The effluents were collected, put into fridge below 4 ^{o}C and analyzed immediately. The results shown are the average of duplicates with the corresponding error bars presented. The degradation of the starting NAs during the preheating stage was checked and was always negligible. The stoichiometric doses mentioned in the current work always refer to the starting amount of the corresponding NAs and are calculated according to previous work[12]. In the case of CHA at 50 mg L^{-1}, the stoichiometric amounts are 1673.4 and 239 mg L^{-1} for sodium persulfate and hydrogen peroxide, respectively. The experiments

were carried out without aeration since the amount of oxygen in the upper part of the reactor (where air is enclosed) is in excess respect to the needed according to the reactions for PS-oxidation in presence of O_2 (see supporting information).

Analytical methods

The concentrations of CHA and CHBA were measured by Gas Chromatography with Flame Ionization Detector (GC-FID) in a GC 3900 Varian provided with a 30 m length × 0.25 mm i.d. capillary column (CP-Wax 52 CB, Varian) using nitrogen as carrier gas. For CHA, the initial oven temperature was set at 70 ^{o}C and then increased up to 240 ^{o}C at a rate of 30 ^{o}C min^{-1}. For CHBA, the only difference was lowering the heating rate to 20 ^{o}C min^{-1}. The concentration of cyclohexanone as an intermediate of PS oxidation of CHA was also determined by GC-FID following the method for CHA analysis. 2-NA and 1234-T-2-NA were determined by high-performance liquid chromatography (HPLC; Varian Pro-Start 240) with a UV detector and Microsorb C18 5 μm column (250 × 4.6 mm) as stationary phase. Acetonitrile and 4 mM H_2SO_4 (1/1) were used as mobile phase at an injection rate of 1 mL min^{-1} with the oven temperature set at 60 ^{o}C.

Total organic carbon (TOC) was measured by a TOC analyzer (Shimadzu, mod. TOC VSCH) and PS concentration by a spectrophotometric method based on a modification of the iodometric titration analysis[45]. The concentration of hydrogen peroxide was analyzed by colorimetric titration using the $TiOSO_4$ method[46]. Iron was determined by the o-phenantroline method[47].

Short-chain carboxyl acids by ionic chromatography with chemical suppression (Metrohm 790 IC) using a conductivity detector. A Metrosep A supp 5−250 column (25 cm length, 4 mm i.d.) was used as stationary phase and an aqueous solution of 3.2 mM Na_2CO_3 and 1 mM of $NaHCO_3$ at pumping rate of 0.7 mL min^{-1} as mobile phase.

Chemical oxygen demand (COD) was determined by oxidation with potassium dichromate following the Standard Method (ISO 6060) using UV-vis spectrometer (Shimadzu, mod. UV-1603). BOD_5 measurements were conducted in a Velps Scientifica apparatus using the standard procedure available from previous work[48]. 400 mL samples of the initial or treated NAs were mixed with activated sludge at 75 mg VSS L^{-1} and pH = 7.2 in the presence of phosphate buffer. $CaCl_2$, KCl and $MgSO_4$ were added as micronutrients and 1.25 mg L^{-1} N-allylthiourea was used as nitrification inhibitor. The biodegradability index was calculated as the BOD_5/COD ratio[19]. The data of BOD_5 and COD were averages of triplicates with error bars.

A well-developed respirometric test was carried out for the assessment of the biodegradability before and after treatment. A LSS respirometer was used with intermittent aeration during 72 h[49, 50]. Two limited values of oxygen concentration were set lower than water-solubility at the given conditions. Each specific oxygen uptake rate (SOUR) data was recorded once the amount of dissolved oxygen dropped to the bottom limit due to the microbial respiration. In the meantime, the aeration was started, and then stopped until the oxygen concentration reached the upper limit. A biomass concentration of 350 mg VSS L^{-1} was used according to the preliminary tests. The reactors were placed in a thermostatic water bath at 25 ^{o}C with magnetic stirring at 500 rpm.

RESULTS AND DISCUSSION

CHA mineralization by conventional Fenton oxidation was firstly checked at initial pH = 3 and 80 ^{o}C with 40% and 100% of the stoichiometric amount of H_2O_2 and 5 mg L^{-1} Fe^{2+}. The results are shown in Fig. 1 together with those obtained upon PS only (20% of the stoichiometric amount) and PS/H_2O_2 simultaneous oxidation (20% and 40%

of the stoichiometric for PS and H_2O_2 respectively) at the same temperature and initial pH = 8.

Fairly poor mineralization (≈ 18%) was achieved by only Fenton oxidation even using H_2O_2 at 239 mg L^{-1} (i.e. 100% of the stoichiometric). Slow decomposition of H_2O_2 was observed (≈ 25%, after 6 h of reaction) associated to a continuous reduction of the measured Fe concentration down to less than 1 mg L^{-1} whereas the pH was still at the optimum value for the Fenton process (≈ 3). These poor results be due to the complexation of Fe by CHA[41]. On the other hand, PS oxidation yielded 40% mineralization at 20% of the stoichiometric amount. Simultaneous PS/Fenton oxidation (initial pH value is also at 8) with PS and H_2O_2 at 20% and 40% of the stoichiometric, respectively, led to only slightly higher mineralization than the sole PS at the same dose (20%), in spite that certain synergistic effect has been reported by other authors in PS/H_2O_2 oxidation[51, 52].

Two-step PS and Fenton oxidation

Based on the important pH reduction caused by PS oxidation, a combination of PS and subsequent Fenton oxidation was investigated. The amount of PS as well as the reaction time in the PS oxidation step will affect to the pH and composition of the resulting effluent which enters the following Fenton oxidation step. Different experiments were performed using 1, 5, 10 and 20% of the stoichiometric PS with CHA at 50 mg L^{-1} and 2 h reaction time, followed by Fenton oxidation with 95.6 mg L^{-1} of H_2O_2 (40% of the stoichiometric) and 5 mg L^{-1} Fe^{2+}.

The results are shown in Fig. 2(a), where it can be seen the important effect of increasing the PS dose within the range tested. Below 10% of the stoichiometric, the subsequent Fenton step had no significant effect. Beyond that PS dose, further Fenton

oxidation became increasingly efficient while effective H_2O_2 decomposition was observed and the measured Fe concentration remained stable in the vicinity of 5 mg L^{-1}. This can be explained by the pre-degradation extent of CHA so that iron naphthenate complexes are not formed, but also by the fact that the pH of the effluent from the PS step approached to the optimum for Fenton oxidation (≈ 3) as the PS dose was increased. In fact, PS oxidation alone at higher dose of around 35% of the stoichiometric allows achieving 80% mineralization of CHA[12]. Now, the combination with a subsequent Fenton treatment provides a way of reducing the PS needs by 43% by using much cheaper H_2O_2 (the Fenton reagent) while still maintaining the mineralization percentage close to the above value. The remaining TOC in the current system corresponds to short-chain organic acids of very low significance in terms of toxicity. It is true that the reduction of the PS amount is accompanied by a complementary addition of H_2O_2 to accomplish further Fenton oxidation, so the amount of H_2O_2 must be conveniently adjusted to minimize total reagent consumption.

Fig. 2(b) shows the results obtained with different H_2O_2 doses in the Fenton step expressed as percent of the theoretical stoichiometric amount relative to initial CHA. The PS amount in the previous step was always 20% of the stoichiometric. As can be seen, the extent of mineralization in the Fenton step increased significantly with the H_2O_2 dose up to around 30% of the stoichiometric and then the remaining TOC (corresponding mostly to short-chain organic acids) seems refractory to Fenton oxidation. Increasing the Fe^{2+} dose above 5 mg L^{-1} neither showed any significant effect on the Fenton step.

The duration of the PS step was also varied since it can affect to the extent of CHA breakdown and consequently to the evolution of TOC upon further Fenton oxidation. Fig. 2(c) shows the results obtained at different duration of the PS step. As can be seen,

the overall TOC removal of the combined system decreased significantly when PS oxidation lasted less than 1.5-2 h.

Finally, the effect of initial pH was studied within the range of 3 to 12, using 20% of the stoichiometric amount of PS in the first step and 40% of the stoichiometric H_2O_2 with 5 mg L^{-1} Fe^{2+} in the subsequent Fenton. Previous studies indicated that pH value of solution can impact on the efficiency of PS oxidation of organic pollutants, since it is associated with the formation of $HO^{\bullet}$ radicals from the reaction of $SO_4^{\bullet-}$ and OH^-[53-55]. Higher pH value is supposed to allow a positive impact to some extent[55], but some adverse effect has also been observed when the pH value reaches above 9[53]. In the current study, the pH was not artificially controlled so that it decreased automatically due to the release of protons from the reaction between PS and NAs[12]. As can be observed in Fig. 2(d), the initial pH had no significant effect on CHA mineralization, given the fact that the pH evolved always to around 3 in the PS oxidation step. Therefore, this two-step PS and Fenton system does not need any artificial correction of the initial pH of the wastewater to be treated.

Summarizing, the combined PS and Fenton system shows significant advantage compared to the only thermally-activated PS and to Fenton oxidation. It mineralizes close to 80% of CHA (50 mg L^{-1}) working at 80 ^oC (thermally-activated PS) with PS and H_2O_2 at 20 and 30% of the stoichiometric amount, respectively. That represents ≈ 335 mg L^{-1} of sodium PS and 75 mg L^{-1} of H_2O_2 (plus 5 mg L^{-1} Fe^{2+}) in terms of reagents consumption. Fenton alone is far from achieving that objective even at high H_2O_2 doses (100% of the stoichiometric) whereas PS oxidation by itself would require around 35% of the stoichiometric amount, i.e. ≈ 586 mg L^{-1} of sodium PS. Therefore, about 251 mg L^{-1} sodium PS are substituted by ≈ 75 mg L^{-1} of H_2O_2 in the combined treatment. At average industrial prices of around 1100 \$ t^{-1} for the former, 250 \$ t^{-1} for H_2O_2 (35%

solution) and 46 \$ t^{-1} for $FeSO_4 \cdot 7H_2O$, the combined treatment system means a significantly lower cost in terms of reagent consumption (≈ 35% overall reduction). Also, it has the additional advantage of significantly lower sulfate and sodium concentration in the final effluent. As additional consideration, it must be taken into account that the working temperature (80 ^oC for thermal PS activation) is around that of OSPWs[43], which further emphasizes the potential application of this combined system to those effluents.

Kinetic analysis

The previous studies on the kinetics of NAs degradation based mainly on the evolution of concentration of the starting compound but regardless of possible intermediates at the risk of an increase in toxicity, which should be importantly considered. In that respect, the TOC (mineralization)-based kinetics allows learning on the complete depletion of organic compounds upon the reaction. Simple pseudo-first-order equation has been used in our previous research to simulate the evolution of NAs mineralization. The current study further improves the kinetic model by considering both the time-course of mineralization and the oxidizing reagents including persulfate and H_2O_2 in both the two steps. The rates of PS and H_2O_2 decomposition in each corresponding step, respectively, can be expressed by first-order kinetics:

$$-\frac{dC_{PS}}{dt} = k_{PS}C_{PS} \qquad (E1)$$

$$-\frac{dC_{H_2O_2}}{dt} = k_{H_2O_2}C_{H_2O_2} \qquad (E2)$$

where C_{PS} and $C_{H_2O_2}$ represent the concentrations of PS and H_2O_2, respectively and k_{PS} and $k_{H_2O_2}$ the corresponding rate constants.

Oxygen can be considered in excess with respect to the reactants at the working conditions, so that its effect can be assumed as invariable during the PS stage. For TOC removal, the following equation is proposed:

$$-\frac{dC_{TOC}}{dt} = k_1 C_{TOC} C_{PS} + k_2 C_{TOC}^2 C_{H_2O_2} \qquad (E3)$$

where C_{TOC} is the concentrations of TOC, and k_1 and k_2 are the apparent rate constants of mineralization in the PS and Fenton oxidation steps, respectively. As aforementioned, mineralization of NAs with PS has been well described by a first-order rate equation[12] whereas second-order dependence has been used in the literature for phenol mineralization upon Fenton oxidation[38]. Scientist 3.0 software was used to fit the experimental data to equation (E3) by conducting Least Squares Fit with iteration[56].

The results are shown in Fig. 3, where fairly good fitting can be corroborated. The values of the corresponding apparent rate constants are listed in Table 1 together with the correlation coefficients. A difference of two orders of magnitude among the rate constants at 60 and 97 ^oC can be observed, suggesting that the system is quite temperature-dependent. The Arrhenius plots are depicted in Fig. 4. A value of 115 kJ mol^{-1} (r^2 = 0.998) was obtained for the apparent activation energy of the PS oxidation step and 87 kJ mol^{-1} for the Fenton one (in this case, the value of the rate constant at 60 ^oC was not considered since desirable pH for Fenton was not achieved working at that temperature).

Table 1 Values of the apparent rate constants of CHA mineralization upon PS and Fenton oxidation at different working temperatures. PS and H_2O_2 at 20 and 40% of the stoichiometric, respectively; Fe^{2+} at 5 mg L^{-1}.

T	PS stage				Fenton stage			
(^oC)	$k_1 \times 10^5$ L mg^{-1} min^{-1}	r^2	$k_{PS} \times 10^2$ min^{-1}	r^2	$k_2 \times 10^5$ L^2 mg^{-2} min^{-1}	r^2	$k_{H_2O_2} \times 10^2$ min^{-1}	r^2

97	13.9±3.22	0.992	7.98±0.43	0.995	10.4±2.47	0.978	20.4±2.46	0.999
90	7.19±1.57	0.998	4.56±0.10	0.999	6.33±2.54	0.972	12.6±2.91	0.999
80	2.46±1.25	0.998	1.56±0.12	0.993	2.74±0.54	0.988	4.18±0.61	0.975
70	0.669±0.32	1.000	0.798±0.04	0.998	1.14±0.61	0.998	2.46±0.35	0.967
60	0.239±0.15	1.000	0.521±0.02	0.999	0.065±0.04	1.000	1.41±0.22	0.965

Degradation of other NAs

The other individual NAs, namely CHBA, 2-NA and 1234-T-2-NA, as well as a mixture of them (including CHA), were tested. As indicated before, these NAs include saturated-ring as well as aromatic structures. The amounts of PS and H_2O_2 used for the treatment of the NAs mixture were calculated according to the proportion of each NA. As can be seen from Fig. 5, the mineralization efficiency was significantly improved after the addition of Fenton reagent in all cases. The corresponding rate constants are collected in Table 2. Regarding the NAs mixture, it is remarkable that the extent of mineralization was close to the observed for the most reactive ones, suggesting some kind of synergistic effect which requires further research given its importance to cope with the complexity of real OSPWs. Further efforts must be addressed to evaluate the efficiency of the combined method proposed toward real oil sands affected-wastewaters containing NAs.

Table 2 Values of the apparent rate constants for the PS and Fenton oxidation of individual NAs and mixture of them. PS and H_2O_2 at 20 and 40% of the stoichiometric, respectively. Fe^{2+} = 5 mg L^{-1}; T = 80 ^oC.

	PS stage				Fenton stage			
NAs	$k_1 \times 10^5$ L mg^{-1} min^{-1}	r^2	$k_{PS} \times 10^2$ min^{-1}	r^2	$k_2 \times 10^5$ L^2 mg^{-2} min^{-1}	r^2	$k_{H_2O_2} \times 10^2$ min^{-1}	r^2

CHBA	2.91±0.23	0.998	1.84±0.16	0.991	5.51±1.54	0.976	4.22±0.58	0.992
2-NA	0.482±0.12	1.000	1.13±0.14	0.986	7.79±0.38	1.000	5.29±0.64	0.986
1234-T-2-NA	0.699±0.25	1.000	1.02±0.17	0.987	6.31±0.32	0.999	5.12±0.59	0.987
Mixed	1.50±0.22	0.999	1.58±0.19	0.985	5.95±1.58	0.987	4.98±0.71	0.980

Evolution of the NAs and oxidation byproducts upon two-step PS and Fenton oxidation

Fig. 6 provides the time-course of NAs upon oxidation by thermally-activated PS with 20% of the stoichiometric amount. As can be observed, that PS dose was enough to achieve complete conversion of the four model NAs tested. However, the results show that the aromatic ring-bearing NAs, namely 2-NA and 1234-T-2-NA, are more resistant to oxidation than the saturated ring-bearing ones (CHA and CHBA). Several oxidation by-products were identified, mainly short-chain organic acids from ring-opening. In all cases, fumaric acid appears as the primary product from the ring-opening and evolves to formic, acetic and oxalic, the two latest being refractory to Fenton oxidation under the operating conditions of the experiments.

Fig. 7 shows the carbon balance throughout the two-step treatment. As can be observed, a large proportion of unidentified organic matter (measured as TOC) was found in the earlier oxidation stages (PS step) in all cases, decreasing gradually as oxidation proceeds upon the Fenton step. Apparently, the nature of those species is related to the starting NA, which also affects to the final breakdown. In the case of the two saturated ring-bearing NAs tested, those byproducts appear quite easily oxidizable by Fenton, achieving final mineralization percentages up to 80 and 91% for CHA and CHBA after the 6 h, where the final identified carbon reached 85 and 97%, respectively. On the opposite, in the case of the aromatic ring-bearing NAs, those byproducts are more refractory, giving rise to significantly lower mineralization (48 and 51% for 2-NA

and 1234-T-2-NA, respectively). Thus, only 51 and 63% of carbon could be identified after oxidation. Therefore, it is important to assess the biodegradability of the remaining matter in order to learn on its potential behavior in a further biological treatment.

Biodegradability

Fig. 8 shows the evolution of the BOD_5 and COD values as well as the BOD_5/COD ratio upon the oxidative treatments of the NAs. The amount of PS used was 20% of the stoichiometric and the reaction conditions in the two-step PS/Fenton oxidation were similar to those of the experiments of Fig. 7. Looking at the BOD_5/COD ratio, the starting NAs yielded quite different values, being particularly low in the case of the aromatic ring-bearing ones (2-NA and 1234-T-2-NA). PS oxidation at 20% of the stoichiometric significantly improved the biodegradability, which was further improved upon the later Fenton treatment.

The respirometric profiles serve to learn on the behavior of the oxidation effluents upon further biological treatment[49, 50]. Since fairly low TOC remains after the two-step oxidation approach using the aforementioned doses (PS at 20% of the stoichiometric amount, H_2O_2 at 40 % of the stoichiometric and Fe^{2+} at 5.0 mg L^{-1}), now only 20% of the stoichiometric amount of H_2O_2 was used in the Fenton stage. The results of the respirometric tests with the starting NAs (100 mg L^{-1}) and the effluents from PS oxidation alone and PS+Fenton are depicted in Fig. 9 (for the saturated-ring bearing ones) and Fig. 10 (for the aromatic ones).

Relatively slow sludge respiration of the raw CHA was observed throughout the respirometric test, especially within the earlier stages (inserted graph in Fig. 9) with less than 15% of TOC removed after 72 h. This confirms its bio-recalcitrant character, in agreement with the literature[2] and consistently with the previous value of the

BOD_5/COD ratio. Regarding the effluent from thermally-activated PS oxidation of CHA, the respirometric test showed obvious activity at the beginning with a sharp decline of SOUR within the first 2 hours (corresponding insert graph in Fig. 9), indicating a fast consumption of some readily biodegradable intermediates. The microbial activity was then maintained at slow SOUR and it increased again after around 25 h. Further dramatic decrease occurred at ≈ 65 h, suggesting the recalcitrant character of the degradation byproducts at that point of the respirometric test. Regarding the effluents from the two-step oxidation of NAs, much higher microbial activity can be seen within the initial period of the respirometric tests, but then fairly low values of SOUR were measured given the strong reduction of TOC.

With regard to CHBA, some higher respirometric intensity was registered within the starting period with the effluents from both the thermally-activated PS and the two-step PS and Fenton treatments. However, with the former, no more data could be recorded after a sharp increase of SOUR at around 10 h, suggesting some toxic incidence on the microorganisms since about 60% of the initial TOC was still remaining so that a lack of available carbon source cannot be postulated.

In the case of the aromatic-ring-bearing NAs (2-NA and 1234-T-2-NA), the effluents from the two-step oxidation always showed the best biodegradability within the starting hours, compared with the thermally-activated PS-treated and the original NAs (Fig. 10). The two-step oxidation effluents from those species show almost complete decline of SOUR, most probably due to the almost complete degradation of the TOC remaining after the oxidative treatment.

In summary, the BOD_5/COD values and respirometric profiles provide available information on the biodegradability of the oxidation effluent of NAs tested. Further

efforts are expected to be made on conducting a real biotreatment of the oxidation effluent of NAs to check the actual biodegradability of this kind of wastewaters.

CONCLUSIONS

Two-step PS and Fenton oxidation provides a promising cost-effective approach for the degradation of NAs. About 80% TOC reduction was achieved from CHA (50 mg L^{-1}) with 20 and 30% of the stoichiometric amount of PS and H_2O_2, respectively. This system is much more effective than Fenton oxidation alone and allows reducing the reagent cost with respect to single PS-oxidation while introducing less sulfate in the final effluent. Other individual NAs and their mixture were also tested and high mineralization efficiencies were achieved as well. The remaining TOC corresponded mainly to short-chain organic acids. A simple and practical kinetic model has been proposed, which describes fairly well the time-course of TOC. Values of the rate constants are provided. For CHA mineralization, 115 and 87 kJ mol^{-1} were obtained as representative values of the apparent activation energy for the PS and Fenton oxidation steps, respectively. The effluents from this treatment showed to be easily biodegradable according to the values of the BOD_5/COD ratio and to the observed in the respirometric tests.

ACKNOWLEDGEMENT

We are grateful to the Chinese Scholarship Council (CSC) for supporting the Ph.D. program of Xiyan Xu (CSC, File No. 201308410047). Spanish MINECO is also gratefully acknowledged for the financial support through the project CTQ2013-41963-R.

REFERENCES

1. Sun N, Chelme-Ayala P, Klamerth N, McPhedran KN, Islam MS, Perez-Estrada L, Drzewicz P, Blunt BJ, Reichert M and Hagen M, Advanced Analytical Mass Spectrometric Techniques and Bioassays to Characterize Untreated and Ozonated Oil Sands Process-Affected Water. *Environ. Sci. Techol.* **48**: 11090-11099 (2014).

2. Kannel PR and Gan TY, Naphthenic acids degradation and toxicity mitigation in tailings wastewater systems and aquatic environments: a review. *J. Environ. Sci. Health. A* **47**: 1-21 (2012).

3. Niasar HS, Li H, Kasanneni TVR, Ray MB and Xu CC, Surface amination of activated carbon and petroleum coke for the removal of naphthenic acids and treatment of oil sands process-affected water (OSPW). *Chem. Eng. J.***293**: 189-199 (2016).

4. Shah SN, Chellappan LK, Gonfa G, Mutalib MIA, Pilus RBM and Bustam MA, Extraction of naphthenic acid from highly acidic oil using phenolate based ionic liquids. *Chem. Eng. J.***284**: 487-493 (2016).

5. Wan Y, Wang B, Khim JS, Hong S, Shim WJ and Hu J, Naphthenic acids in coastal sediments after the Hebei Spirit oil spill: a potential indicator for oil contamination. *Environ. Sci. Techol.* **48**: 4153-4162 (2014).

6. Clemente JS and Fedorak PM, A review of the occurrence, analyses, toxicity, and biodegradation of naphthenic acids. *Chemosphere* **60**: 585-600 (2005).

7. Zhang X, Wiseman S, Yu H, Liu H, Giesy JP and Hecker M, Assessing the toxicity of naphthenic acids using a microbial genome wide live cell reporter array system. *Environ. Sci. Techol.* **45**: 1984-1991 (2011).

8. Tollefsen KE, Petersen K and Rowland SJ, Toxicity of synthetic naphthenic acids and mixtures of these to fish liver cells. *Environ. Sci. Techol.* **46**: 5143-5150 (2012).

9. Drzewicz P, Perez-Estrada L, Alpatova A, Martin JW and El-Din MG, Impact of Peroxydisulfate in the Presence of Zero Valent Iron on the Oxidation of Cyclohexanoic Acid and Naphthenic Acids from Oil Sands Process-Affected Water. *Environ. Sci. Techol.* **46**: 8984-8991 (2012).

10. Purcell JM, Juyal P, Kim D-G, Rodgers RP, Hendrickson CL and Marshall AG, Sulfur speciation in petroleum: Atmospheric pressure photoionization or chemical derivatization and electrospray ionization Fourier transform ion cyclotron resonance mass spectrometry. *Energy & Fuels* **21**: 2869-2874 (2007).

11. Quinlan PJ and Tam KC, Water treatment technologies for the remediation of naphthenic acids in oil sands process-affected water. *Chem. Eng. J.***279**: 696-714 (2015).

12. Xu X, Pliego G, Zazo JA, Casas JA and Rodriguez JJ, Mineralization of naphtenic acids with thermally-activated persulfate: The important role of oxygen. *J. Hazard. Mater.* **318**: 355-362 (2016).

13. Zhang Y, Xue J, Liu Y and El-Din MG, Treatment of oil sands process-affected water using membrane bioreactor coupled with ozonation: A comparative study. *Chem. Eng. J.***302**: 485-497 (2016).

14. Xu X, Pliego G, Zazo JA, Sun S, GarcÍa-muÑoz P, He L, Casas JA and Rodriguez JJ, An overview on the application of advanced oxidation processes for the removal of naphthenic acids from water. *Crit. Rev. Environ. Sci. Tec.* **47**: 1337–1370 (2017).

15. Iranmanesh S, Harding T, Abedi J, Seyedeyn-Azad F and Layzell DB, Adsorption of naphthenic acids on high surface area activated carbons. *J. Environ. Sci. Health. A* **49**: 913-922 (2014).

16. Gunawan Y, Nemati M and Dalai A, Biodegradation of a surrogate naphthenic acid under denitrifying conditions. *Water Res.* **51**: 11-24 (2014).

17. Drzewicz P, Afzal A, El-Din MG and Martin JW, Degradation of a model naphthenic acid, cyclohexanoic acid, by vacuum UV (172 nm) and UV (254 nm)/H2O2. *J. Phys. Chem. A* **114**: 12067-12074 (2010).

18. Liang X, Zhu X and Butler EC, Comparison of four advanced oxidation processes for the removal of naphthenic acids from model oil sands process water. *J. Hazard. Mater.* **190**: 168-176 (2011).

19. Xu X-Y, Zeng G-M, Peng Y-R and Zeng Z, Potassium persulfate promoted catalytic wet oxidation of fulvic acid as a model organic compound in landfill leachate with activated carbon. *Chem. Eng. J.***200**: 25-31 (2012).

20. Zazo JA, Casas JA, Mohedano AF and Rodríguez JJ, Catalytic wet peroxide oxidation of phenol with a Fe/active carbon catalyst. *Appl. Catal. B-Environ.* **65**: 261-268 (2006).

21. Rodriguez S, Vasquez L, Costa D, Romero A and Santos A, Oxidation of Orange G by persulfate activated by Fe(II), Fe(III) and zero valent iron (ZVI). *Chemosphere* **101**: 86-92 (2014).

22. Do S-H, Kwon Y-J, Bang S-J and Kong S-H, Persulfate reactivity enhanced by Fe 2 O 3–MnO and CaO–Fe 2 O 3–MnO composite: Identification of composite and degradation of CCl 4 at various levels of pH. *Chem. Eng. J.***221**: 72-80 (2013).

23. Ji Y, Shi Y, Dong W, Wen X, Jiang M and Lu J, Thermo-activated persulfate oxidation system for tetracycline antibiotics degradation in aqueous solution. *Chem. Eng. J.***298**: 225-233 (2016).

24. Umar M, Roddick F and Fan L, Effect of coagulation on treatment of municipal wastewater reverse osmosis concentrate by UVC/H_2O_2. *J. Hazard. Mater.* **266**: 10-18 (2014).

25. Khan JA, He X, Shah NS, Khan HM, Hapeshi E, Fatta-Kassinos D and Dionysiou DD, Kinetic and mechanism investigation on the photochemical degradation of atrazine with activated H_2O_2, $S_2O_8^{2-}$ and HSO_5^-. *Chem. Eng. J.* **252**: 393-403 (2014).

26. Pliego G, Xekoukoulotakis N, Venieri D, Zazo JA, Casas JA, Rodriguez JJ and Mantzavinos D, Complete degradation of the persistent anti‐depressant sertraline in aqueous solution by solar photo‐Fenton oxidation. *J. Chem. Technol. Biotechnol.* **89**: 814-818 (2014).

27. Umar M, Roddick F, Fan L, Autin O and Jefferson B, Treatment of municipal wastewater reverse osmosis concentrate using UVC-LED/H_2O_2 with and without coagulation pre-treatment. *Chem. Eng. J.* **260**: 649-656 (2015).

28. Yuan S, Liao P and Alshawabkeh AN, Electrolytic manipulation of persulfate reactivity by iron electrodes for trichloroethylene degradation in groundwater. *Environ. Sci. Techol.* **48**: 656-663 (2014).

29. Garcia-Garcia E, Ge JQ, Oladiran A, Montgomery B, El-Din MG, Perez-Estrada LC, Stafford JL, Martin JW and Belosevic M, Ozone treatment ameliorates oil sands process water toxicity to the mammalian immune system. *Water research* **45**: 5849-5857 (2011).

30. Zhang Y, Klamerth N and El-Din MG, Degradation of a model naphthenic acid by nitrilotriacetic acid–modified Fenton process. *Chem. Eng. J.* **292**: 340-347 (2016).

31. Leshuk T, Wong T, Linley S, Peru K, Headley J and Gu F, Solar photocatalytic degradation of naphthenic acids in oil sands process-affected water. *Chemosphere* **144**: 1854-1861 (2015).

32. Shu Z, Li C, Belosevic M, Bolton JR and El-Din MG, Application of a Solar UV/Chlorine Advanced Oxidation Process to Oil Sands Process-Affected Water Remediation. *Environ. Sci. Techol.* **48**: 9692-9701 (2014).

33. Madhavan V, Levanon H and Neta P, Decarboxylation by SO4-radicals. *Radiation Research* **76**: 15-22 (1978).

34. Fang G, Gao J, Dionysiou DD, Liu C and Zhou D, Activation of persulfate by quinones: Free radical reactions and implication for the degradation of PCBs. *Environ. Sci. Techol.* **47**: 4605-4611 (2013).

35. Peyton GR, The free-radical chemistry of persulfate-based total organic carbon analyzers. *Marine Chemistry* **41**: 91-103 (1993).

36. Liu H, Bruton TA, Li W, Buren JV, Prasse C, Doyle FM and Sedlak DL, Oxidation of benzene by persulfate in the presence of Fe (III)-and Mn (IV)-containing oxides: stoichiometric efficiency and transformation products. *Environ. Sci. Techol.* **50**: 890-898 (2016).

37. Pignatello JJ, Oliveros E and MacKay A, Advanced oxidation processes for organic contaminant destruction based on the Fenton reaction and related chemistry. *Crit. Rev. Environ. Sci. Tec.* **36**: 1-84 (2006).

38. Bautista P, Mohedano A, Casas J, Zazo J and Rodriguez J, An overview of the application of Fenton oxidation to industrial wastewaters treatment. *J. Chem. Technol. Biotechnol.* **83**: 1323-1338 (2008).

39. Zazo JA, Pliego G, Blasco S, Casas JA and Rodriguez JJ, Intensification of the Fenton process by increasing the temperature.Ind. Eng. Chem. Res. **50**: 866-870 (2010).

40. Pliego G, Zazo JA, Casas JA and Rodriguez JJ, Fate of iron oxalates in aqueous solution: The role of temperature, iron species and dissolved oxygen. *J. Environ. Chem. Eng.* **2**: 2236-2241 (2014).

41. Laredo GC, López CR, Alvarez RE and Cano JL, Naphthenic acids, total acid number and sulfur content profile characterization in Isthmus and Maya crude oils. *Fuel* **83**: 1689-1695 (2004).

42. Barona JF, Morales DF, González-Bahamón LF, Pulgarín C and Benítez LN, Shift from heterogeneous to homogeneous catalysis during resorcinol degradation using the solar photo-Fenton process initiated at circumneutral pH. *Appl. Catal. B-Environ.* **165**: 620-627 (2015).

43. Zhang Y, Klamerth N, Messele SA, Chelme-Ayala P and El-Din MG, Kinetics study on the degradation of a model naphthenic acid by ethylenediamine-N, N'-disuccinic acid-modified Fenton process. *J. Hazard. Mater.* **318**: 371-378 (2016).

44. Hong PA, Cha Z, Zhao X, Cheng C-J and Duyvesteyn W, Extraction of bitumen from oil sands with hot water and pressure cycles. *Fuel Process. Techn.* **106**: 460-467 (2013).

45. Liang C, Huang C-F, Mohanty N and Kurakalva RM, A rapid spectrophotometric determination of persulfate anion in ISCO. *Chemosphere* **73**: 1540-1543 (2008).

46. Eisenberg G, Colorimetric determination of hydrogen peroxide. *I nd. Eng. Chem., Anal. Ed.* **15**: 327-328 (1943).

47. Sandell EB, Colorimetric determination of traces of metals. *Interscience Pubs* **New York** (1959).

48. Sanchis S, Polo AM, Tobajas M, Rodriguez JJ and Mohedano AF, Degradation of chlorophenoxy herbicides by coupled Fenton and biological oxidation. *Chemosphere* **93**: 115-122 (2013).

49. Sanchis S, Polo A, Tobajas M, Rodriguez J and Mohedano A, Coupling Fenton and biological oxidation for the removal of nitrochlorinated herbicides from water. *Water Res.* **49**: 197-206 (2014).

50. Polo A, Tobajas M, Sanchis S, Mohedano A and Rodriguez J, Comparison of experimental methods for determination of toxicity and biodegradability of xenobiotic compounds. *Biodegradation* **22**: 751-761 (2011).

51. Liang C, Guo Y-Y and Pan Y-R, A study of the applicability of various activated persulfate processes for the treatment of 2, 4-dichlorophenoxyacetic acid. *Int. J. Environ. Sci. Techol.* **11**: 483-492 (2014).

52. Hilles AH, Amr SSA, Hussein RA, El-Sebaie OD and Arafa AI, Performance of combined sodium persulfate/H 2 O 2 based advanced oxidation process in stabilized landfill leachate treatment. *J. Environ. Manage.* **166**: 493-498 (2016).

53. Criquet J and Leitner NKV, Degradation of acetic acid with sulfate radical generated by persulfate ions photolysis. *Chemosphere* **77**: 194-200 (2009).

54. Liang C, Wang Z-S and Bruell CJ, Influence of pH on persulfate oxidation of TCE at ambient temperatures. *Chemosphere* **66**: 106-113 (2007).

55. Furman OS, Teel AL and Watts RJ, Mechanism of base activation of persulfate. *Environ. Sci. Techol.* **44**: 6423-6428 (2010).

56. Zazo J, Casas J, Mohedano A and Rodriguez J, Semicontinuous Fenton oxidation of phenol in aqueous solution. A kinetic study. *Water Res.* **43**: 4063-4069 (2009).

Figure Caption

Fig. 1 CHA mineralization by various oxidation approaches (Fe^{2+} at 5 mg L^{-1} in Fenton; T = 80 ^{o}C).

Fig. 2 Effect of (a) PS amount, (b) H_2O_2 amount, (c) PS step durations and (d) pH value on the two-step PS and Fenton oxidation of CHA (50 mg L^{-1}) at 80 ^{o}C. In a typical run, PS and H_2O_2 are 20% and 40% of the stoichiometric amount, respectively; the duration of PS is 120 min and Fe^{2+} in the Fenton step is 5 mg L^{-1}.

Fig. 3 Experimental (points) and predicted (lines) TOC values vs reaction time at different temperatures. [PS] = 20% of the stoichiometric; [H_2O_2] = 40 % of the stoichiometric; [Fe^{2+}] = 5.0 mg L^{-1}; pH_0 = 8.

Fig. 4 Arrhenius plots for the PS and Fenton mineralization of CHA. The experimental conditions as Fig. 3.

Fig. 5 Mineralization of different NAs and their mixture. [PS] = 20% of the stoichiometric; [H_2O_2] = 40 % of the stoichiometric; [Fe^{2+}] = 5.0 mg L^{-1}; pH_0 = 8; T = 80 ^{o}C.

Fig. 6 Time-course of the NAs and short-chain acids concentrations upon the two-step PS(2 h) and Fenton oxidation. $[NAs]_0$ = 100 mg L^{-1}; [PS] = 20% of the stoichiometric; [H_2O_2] = 40 % of the stoichiometric; [Fe^{2+}] = 5.0 mg L^{-1}; pH_0 = 8; T = 80 ^{o}C.

Fig. 7 Carbon balance during the two-step PS(2 h) and Fenton oxidation. [PS] = 20% of the stoichiometric; [H_2O_2] = 40 % of the stoichiometric; [Fe^{2+}] = 5.0 mg L^{-1}; pH_0 = 8; T = 80 ^{o}C.

Fig. 8 BOD_5 and COD values after reactions at different conditions (bars) and the corresponding BOD_5/COD values (line+symbols).

Fig. 9 Time-course of SOUR (solid symbols) and TOC (open symbols) upon respirometric tests with the starting CHA and CHBA and the effluents from the oxidation treatments. Initial NAs (circles), NAs after thermally-activated PS oxidation (stars) and two-step PS(2 h) and Fenton(2 h) oxidation (triangles). The inset figures

show the profiles within the earlier stages.

Fig. 10 Time-course of SOUR (solid symbols) and TOC (open symbols) upon respirometric tests with the starting 2-NA and 1234-T-2-NA and the effluents from the oxidation treatments. Symbols as in Fig. 9.

Figures

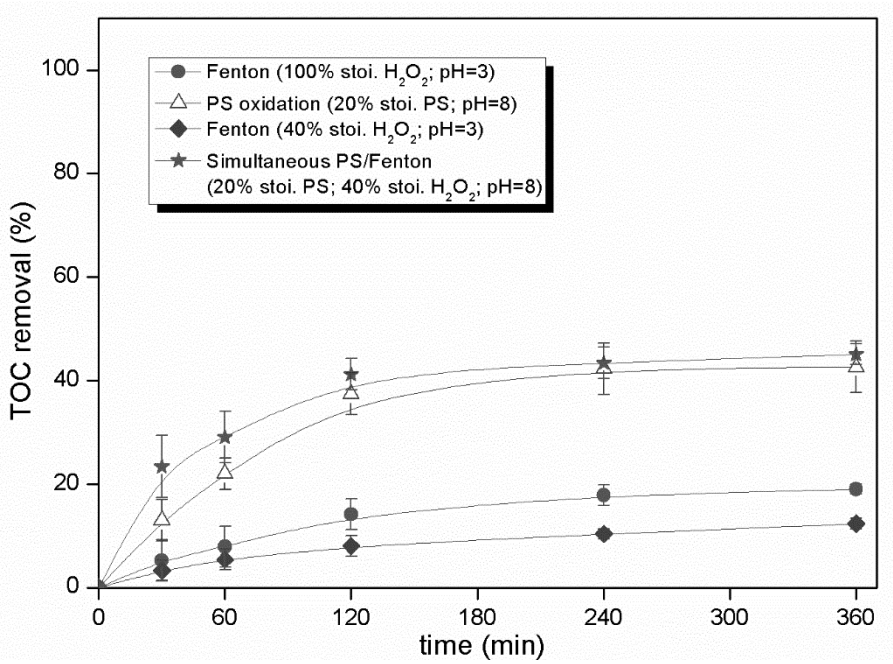

Fig. 1 CHA mineralization by various oxidation approaches (Fe^{2+} at 5 mg L^{-1} in Fenton; T = 80 ^{o}C).

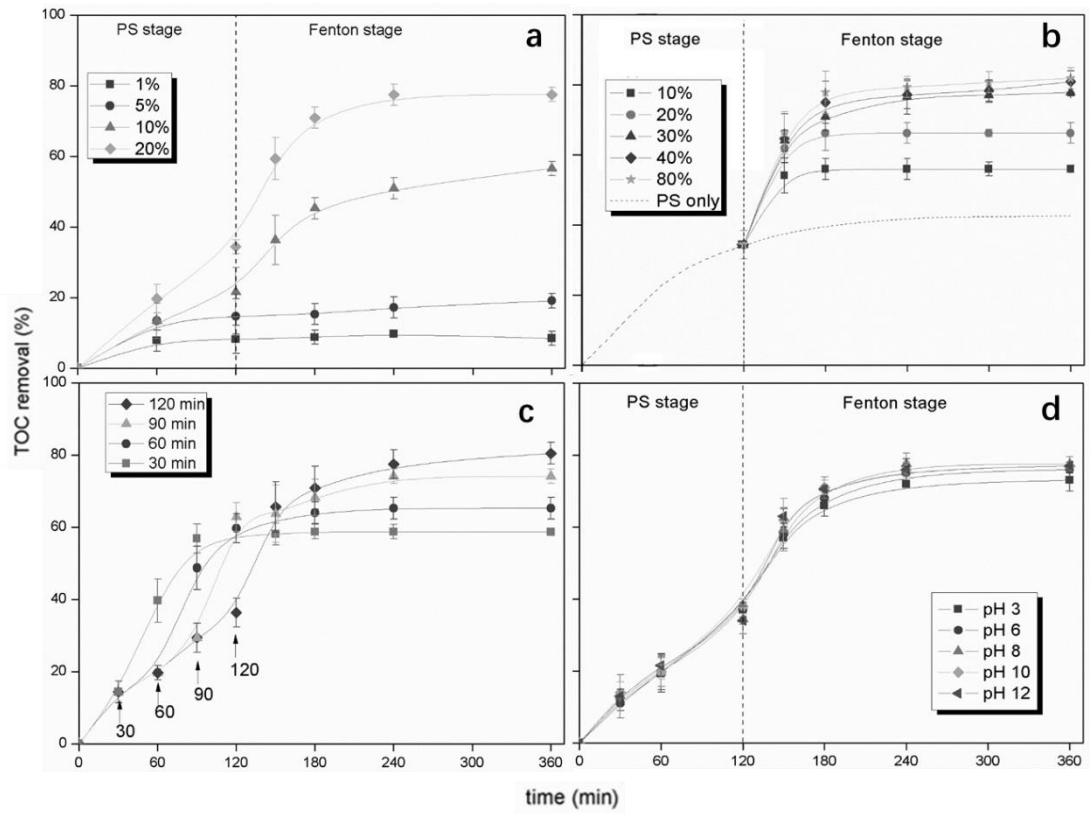

Fig. 2 Effect of (a) PS amount, (b) H_2O_2 amount, (c) PS step durations and (d) pH value on the two-step PS and Fenton oxidation of CHA (50 mg L^{-1}) at 80 ^{o}C. In a typical run, PS and H_2O_2 are 20% and 40% of the stoichiometric amount, respectively; the duration of PS is 120 min and Fe^{2+} in the Fenton step is 5 mg L^{-1}.

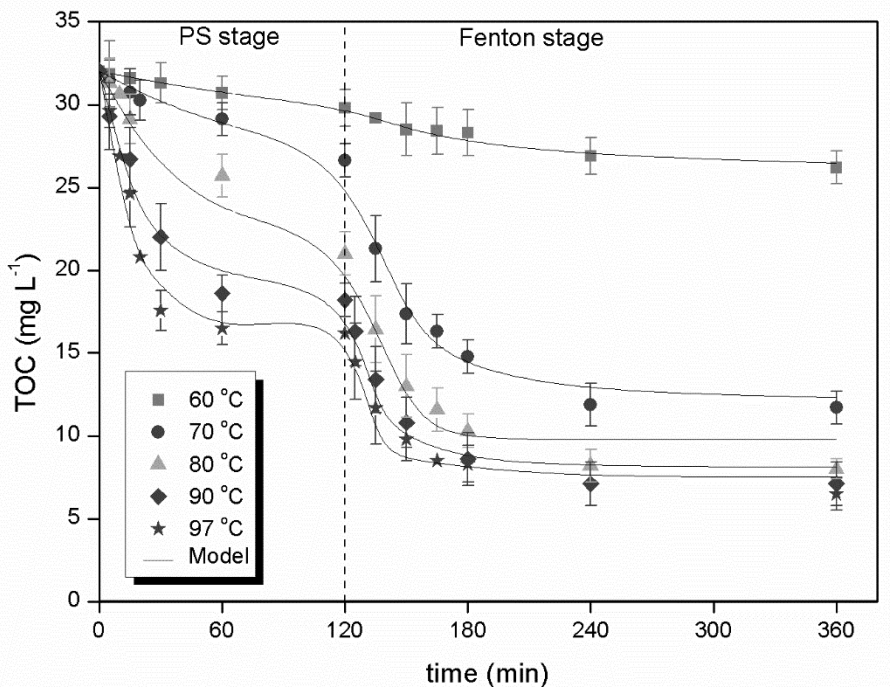

Fig. 3 Experimental (points) and predicted (lines) TOC values vs reaction time at different temperatures. [PS] = 20% of the stoichiometric; [H_2O_2] = 40 % of the stoichiometric; [Fe^{2+}] = 5.0 mg L^{-1}; pH_0 = 8.

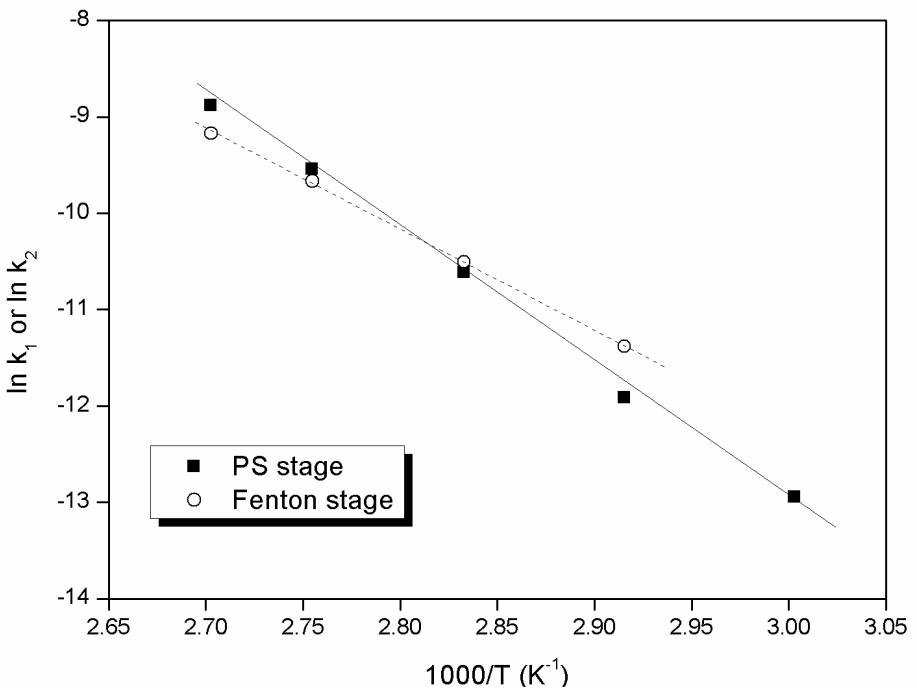

Fig. 4 Arrhenius plots for the PS and Fenton mineralization of CHA. The experimental conditions as Fig. 3.

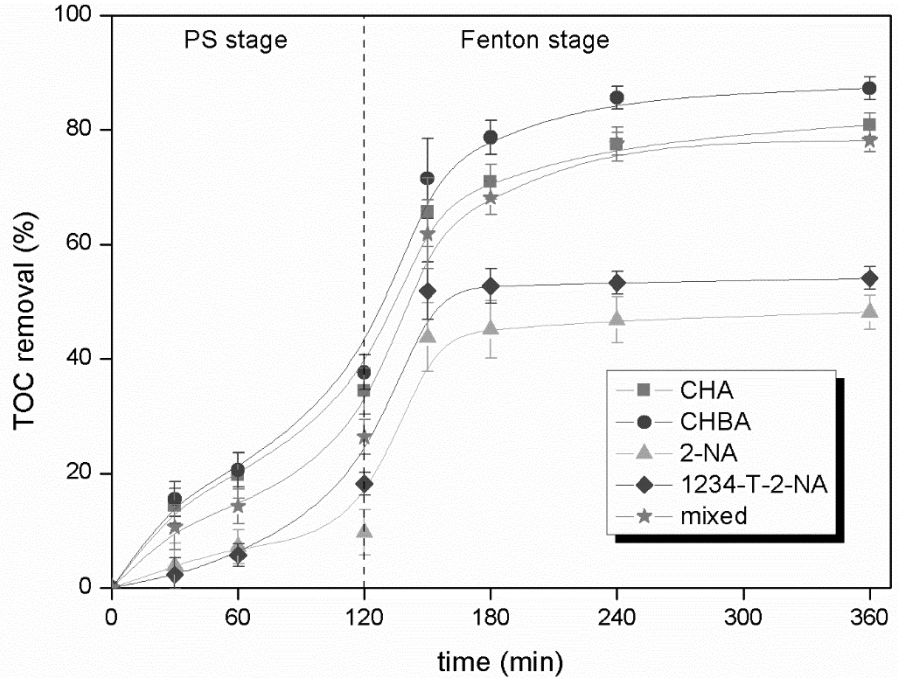

Fig. 5 Mineralization of different NAs and their mixture. [PS] = 20% of the stoichiometric; [H_2O_2] = 40 % of the stoichiometric; [Fe^{2+}] = 5.0 mg L^{-1}; pH_0 = 8; T = 80 ^oC.

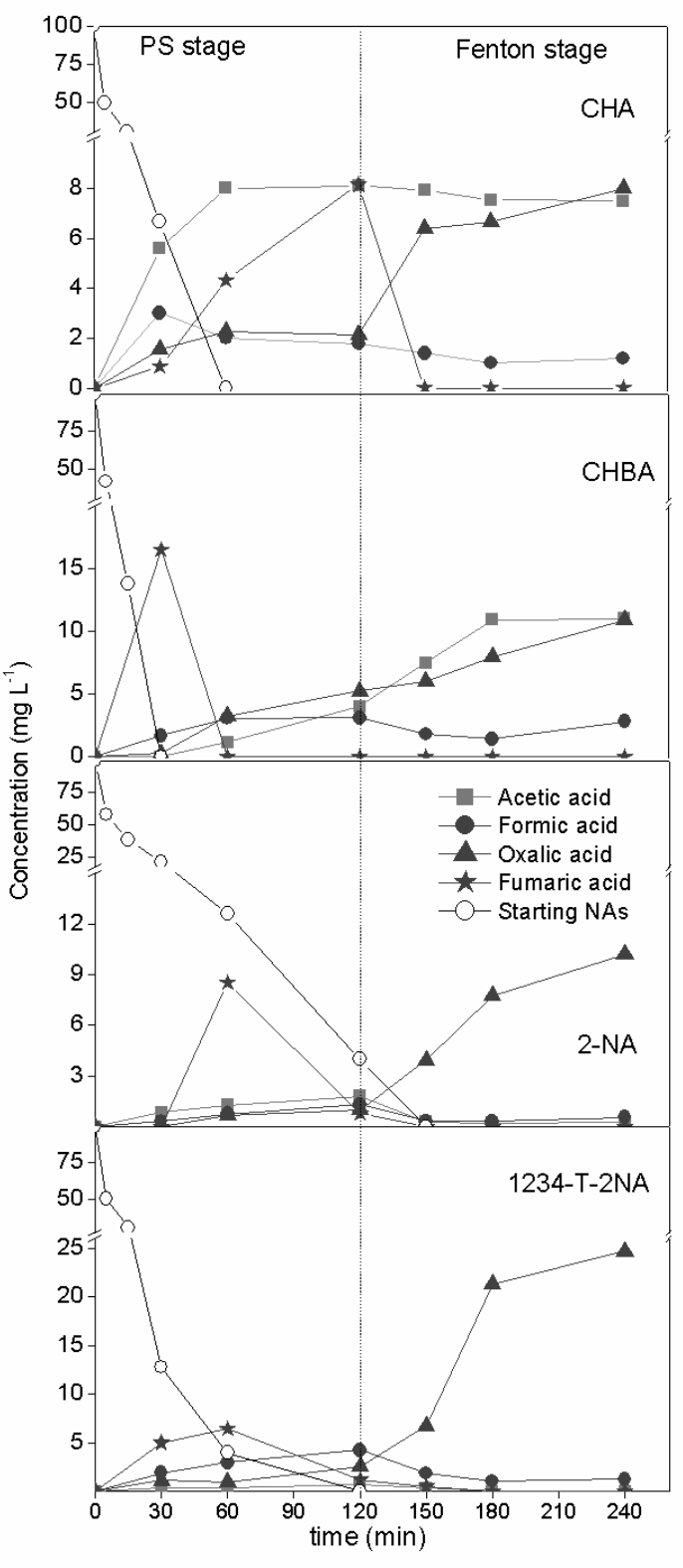

Fig. 6 Time-course of the NAs and short-chain acids concentrations upon the two-step PS(2 h) and Fenton oxidation. $[NAs]_0$ = 100 mg L^{-1}; [PS] = 20% of the stoichiometric; $[H_2O_2]$ = 40 % of the stoichiometric; $[Fe^{2+}]$ = 5.0 mg L^{-1}; pH_0 = 8; T = 80 ^oC.

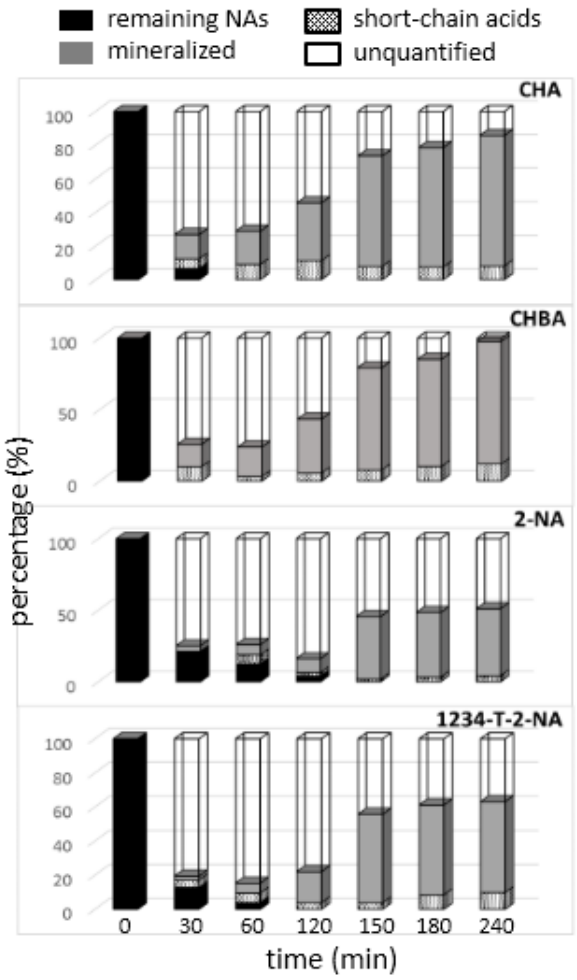

Fig. 7 Carbon balance during the two-step PS(2 h) and Fenton oxidation. [PS] = 20% of the stoichiometric; [H_2O_2] = 40 % of the stoichiometric; [Fe^{2+}] = 5.0 mg L^{-1}; pH_0 = 8; T = 80 ^oC.

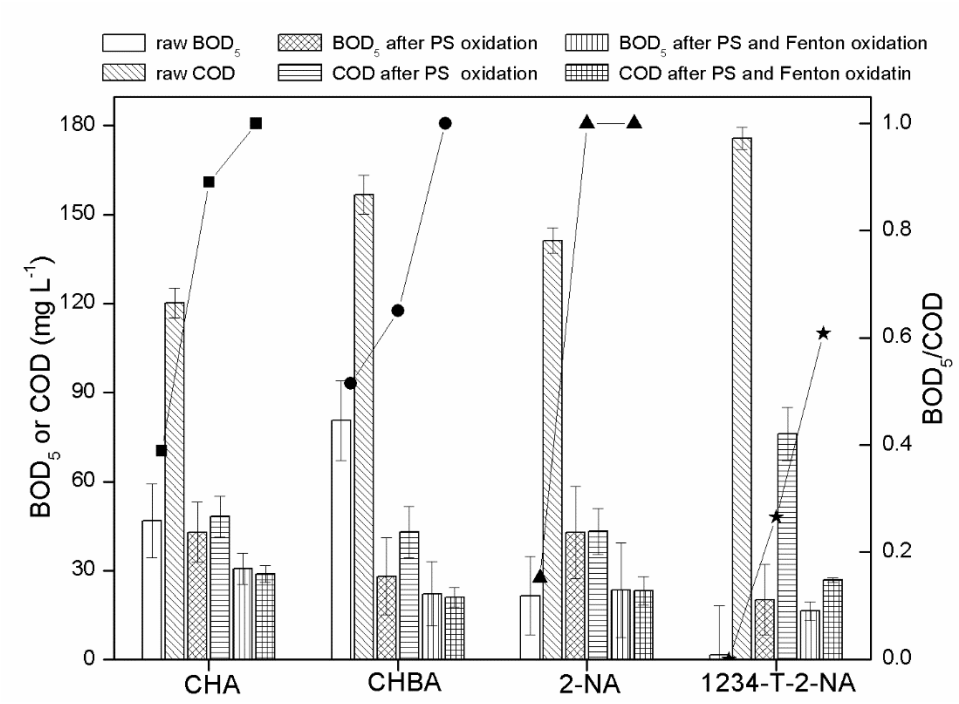

Fig. 8 BOD_5 and COD values after reactions at different conditions (bars) and the corresponding BOD_5/COD values (line+symbols).

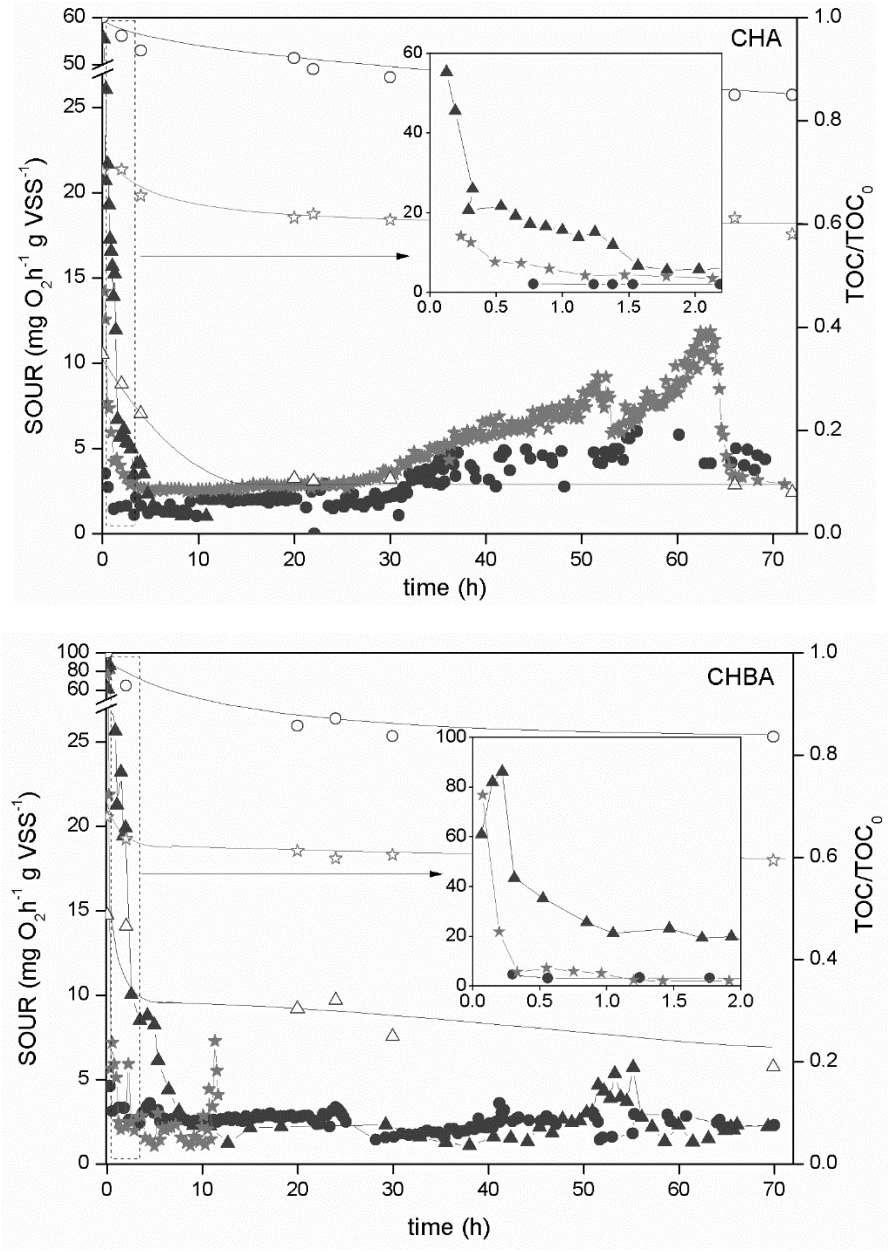

Fig. 9 Time-course of SOUR (solid symbols) and TOC (open symbols) upon respirometric tests with the starting CHA and CHBA and the effluents from the oxidation treatments. Initial NAs (circles), NAs after thermally-activated PS oxidation (stars) and two-step PS(2 h) and Fenton(2 h) oxidation (triangles). The inset figures show the profiles within the earlier stages.

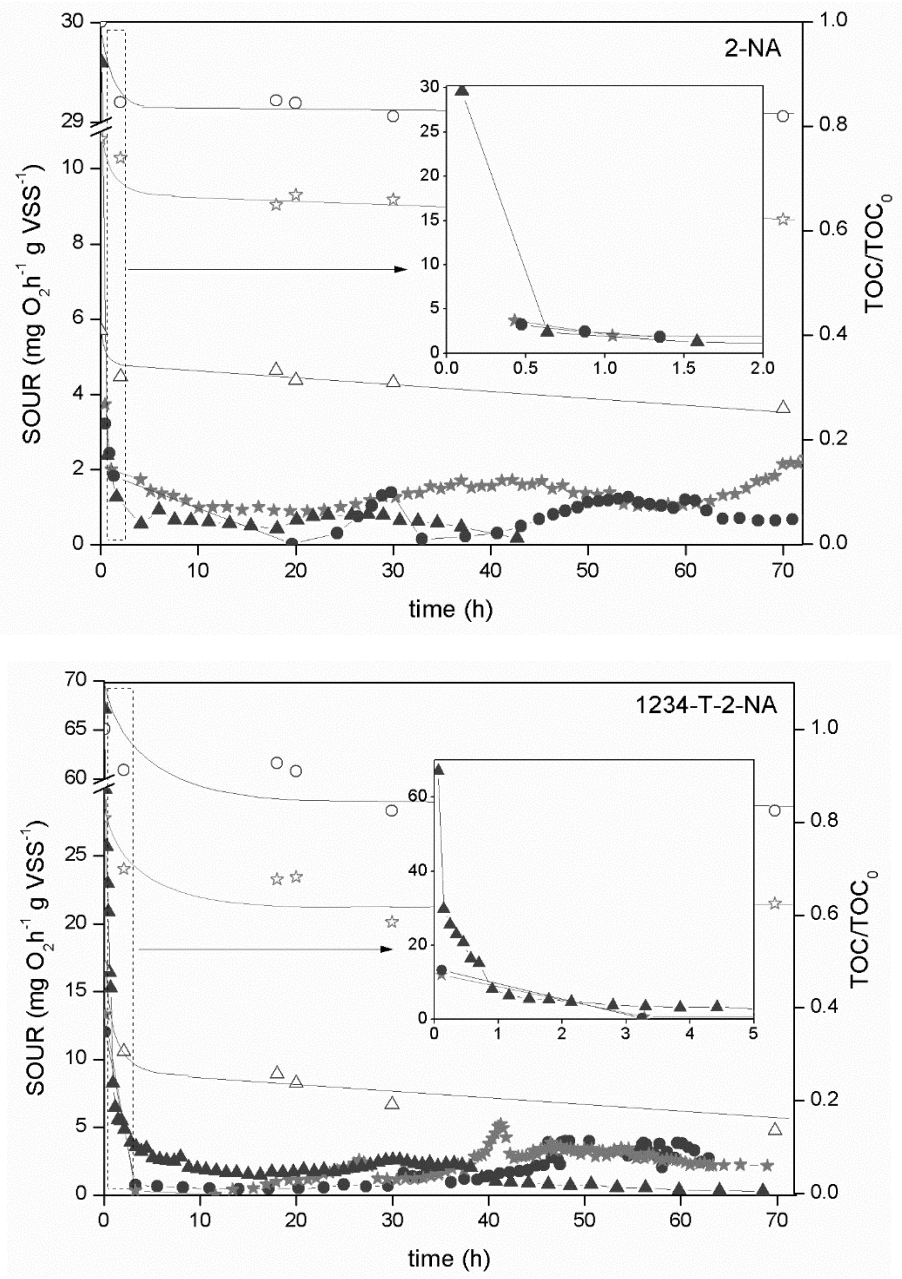

Fig. 10 Time-course of SOUR (solid symbols) and TOC (open symbols) upon respirometric tests with the starting 2-NA and 1234-T-2-NA and the effluents from the oxidation treatments. Symbols as in Fig. 9.